THE JOURNAL OF BIOLOGICAL CHEMISTRY VOL. 282, NO. 40, pp. 29241–29247, October 5, 2007

Structure of Compstatin in Complex with Complement Component C3c Reveals a New Mechanism of Complement Inhibition*[S]

Received for publication, June 4, 2007, and in revised form, July 25, 2007 Published, JBC Papers in Press, August 6, 2007, DOI 10.1074/jbc.M704587200

Bert J. C. Janssen[‡], Els F. Halff[‡], John D. Lambris[§1], and Piet Gros[‡2]

From the [‡]Crystal and Structural Chemistry, Bijvoet Center for Biomolecular Research, Department of Chemistry, Faculty of Sciences, Utrecht University, 3584 CH Utrecht, The Netherlands and the [§]Department of Pathology and Laboratory Medicine, School of Medicine, University of Pennsylvania, Philadelphia, Pennsylvania 19104

Undesired complement activation is a major cause of tissue injury in various pathological conditions and contributes to several immune complex diseases. Compstatin, a 13-residue peptide, is an effective inhibitor of the activation of complement component C3 and thus blocks a central and crucial step in the complement cascade. The precise binding site on C3, the structure in the bound form, and the exact mode of action of compstatin are unknown. Here we present the crystal structure of compstatin in complex with C3c, a major proteolytic fragment of C3. The structure reveals that the compstatin-binding site is formed by the macroglobulin (MG) domains 4 and 5. This binding site is part of the structurally stable MG-ring formed by domains MG 1–6 and is far away from any other known binding site on C3. Compstatin does not alter the conformation of C3c, whereas compstatin itself undergoes a large conformational change upon binding. We propose a model in which compstatin sterically hinders the access of the substrate C3 to the convertase complexes, thus blocking complement activation and amplification. These insights are instrumental for further development of compstatin as a potential therapeutic.

The complement system is a key part of the innate and adaptive immune system and plays a major role in homeostasis by clearing altered host cells and invading pathogens (1, 2). Inappropriate activation of the complement system leads to tissue injury, causing or aggravating various pathological conditions, such as autoimmune diseases, burn injuries, Alzheimer disease, stroke, and heart attack (reviewed in Ref. 3). Several complement inhibitors are under development, targeting various steps in the complement activation pathways. None of these compounds have been approved for clinical use yet (3–5). We studied a 13-residue cyclic peptide, called compstatin, which inhibits complement response by preventing the proteolytic activation of C3 [3] (6). Activation of C3 by the C3 convertases is a central amplification step in complement activation. All three recognition and initiation pathways, the classical, lectin, and alternative pathways, converge in the activation of C3. Proteolytic activation of C3 yields C3b, which covalently binds to pathogenic or self surfaces, providing a strong signal for clearance of the tagged particles. Because compstatin blocks this critical step of complement activation and because it is a small non-immunogenic peptide, compstatin has the potential to be developed into a therapeutic agent.

Compstatin (ICVVQDWGHHRCT-NH_2, circularized by disulfide bond Cys-2–Cys-12) was discovered by a phage-display, random peptide library search (6). Compstatin has been shown to be an effective inhibitor of complement activation in several clinically relevant models (reviewed in Ref. 5). For example, compstatin was shown to prolong the survival of kidneys in an *ex vivo* xenograft model (7), inhibited complement activation during the contact of whole blood with biomaterial in a model of extracorporeal circulation (8), and inhibited *in vivo* complement activation in a non-human primate model of heparin-protamine complex-induced inflammation resembling heart surgery (9). Compstatin displayed an inhibitory activity of $IC_{50} = 12\ \mu M$. In solution, compstatin forms a β-turn at residues Gln-5–Gly-8 with the disulfide bridge Cys-2–Cys-12, residues Ile-1–Val-4, and Thr-13, forming a hydrophobic cluster (10, 11). Mutational studies showed that the polar β-turn and the hydrophobic cluster are essential for the inhibitory activity of compstatin (10–13). Both main-chain and side-chain atoms of compstatin are thought to be involved in interaction with C3 (14). Recently, an analogue of compstatin with 45-fold higher potency was identified, which contained an acetylated N terminus and amino acid substitutions V4W and H9A (Ac-ICVWQDWGAHRCT-NH_2) (15, 16). These compounds bind C3 (K_d of 1.3 and 0.14 μM for natural compstatin

* This work was supported by "Pionier" program Grant 700.99.402 (to P. G.) by the Council for Chemical Sciences of the Netherlands Organization for Scientific Research (NWO-CW) and by National Institutes of Health Grants GM069736, GM62134, and AI30040 (to J. D. L.). The costs of publication of this article were defrayed in part by the payment of page charges. This article must therefore be hereby marked "*advertisement*" in accordance with 18 U.S.C. Section 1734 solely to indicate this fact.

The atomic coordinates and structure factors (code 2QKI) have been deposited in the Protein Data Bank, Research Collaboratory for Structural Bioinformatics, Rutgers University, New Brunswick, NJ (http://www.rcsb.org/).

[S] The on-line version of this article (available at http://www.jbc.org) contains two supplemental tables and two supplemental figures as well as additional references.

[1] To whom correspondence may be addressed. E-mail: lambris@mail.med.upenn.edu.

[2] To whom correspondence may be addressed: Crystal and Structural Chemistry, Bijvoet Center for Biomolecular Research, Faculty of Sciences, Utrecht University, Padualaan 8, 3584 CH Utrecht, The Netherlands. Tel.: 31-30-2533127; Fax: 31-30-2533940; E-mail: p.gros@chem.uu.nl.

[3] The abbreviations used are: C3, complement component 3; MG, macroglobulin; CRIg, complement receptor of the immunoglobulin superfamily; r.m.s., root mean square.

with an acetylated N terminus and the V4W/H9A analogue, respectively (15)) and its derived products C3(H_2O), C3b, and C3c (6, 14). Soulika *et al.* (17) showed that the binding site resides in the 40-kDa C-terminal part of the β-chain that is common to these proteins. Overall, these and other studies have lead to a model in which compstatin inhibits complement activation by blocking binding of C3 to the C3 convertases, either through inducing a conformational change in C3 or through causing steric hindrance when bound to C3 (11, 17).

In the last two years, a wealth of structural data on C3 has become available (18–22). C3 is a two-chain molecule consisting of a β- (residues 1–645) and an α-chain (residues 650–1641) of 75 and 110 kDa, respectively, that are arranged in 13 domains (18). Activation of C3 occurs by cleavage of the scissile bond Arg-726–Ser-727, generating C3a (9 kDa) and C3b (176 kDa) (23). The transformation of C3 into C3b induces large conformational changes in the α-chain (19, 21). In contrast, the β-chain is overall structurally stable. The only exception is the MG3 domain, which is part of the MG-ring, of the β-chain, which shows a reorientation up to 15° when changing from C3 to C3b and C3c (18, 19, 21). The 40-kDa C-terminal fragment, identified by Soulika *et al.* (17), forms part of MG3 and complete MG4, MG5, MG6$^{\beta}$, and the linker domain (18). Thus, compstatin likely binds to the structurally stable part of C3.

We determined the crystal structure of compstatin in complex with C3c to 2.4-Å resolution. We used C3c instead of C3 in these studies because C3c crystallizes more readily than C3 and crystals of C3c diffract to a higher resolution than those of C3. The resulting structure of the C3c-compstatin complex reveals an unexpected binding site and an unexpected conformation of compstatin. Nonetheless, the structure is in agreement with prior observations on the activity of compstatin and its derivatives and explains the species specificity. Using the available structural data, we propose a model for the inhibitory activity of compstatin in blocking substrate C3 binding to C3 convertases.

EXPERIMENTAL PROCEDURES

Protein Purification and Peptide Synthesis—C3c was purified as described previously (18). In brief, C3c from outdated human plasma (stored for several weeks at 4 °C) was purified by polyethylene glycol precipitation, anion-exchange chromatography (DEAE-Sephacel), cation-exchange chromatography (CM-Sephadex C50), and size-exclusion chromatography (Sephacryl 300). C3c was concentrated to 20 mg ml^{-1} and dialyzed against 10 mM Tris, pH 7.4, 2 mM EDTA, and 2 mM benzamidine. For crystallization purposes, the glycan moiety on Asn-917 was cleaved off with *N*-glycosidase F. The improved compstatin analogue (Ac-ICVWQDWGAHRCT-NH_2) displaying 45-fold higher activity when compared with the parent peptide was synthesized and purified as described previously (16) and lyophilized for storage. Prior to crystallization, C3c at 20 mg/ml (0.148 mM) in 10 mM Tris, pH 7.4, 2 mM EDTA, and 2 mM benzamidine was mixed with lyophilized compstatin to a final concentration of 4.8 mg/ml (3.0 mM).

Crystallization and Data Collection—C3c-compstatin was crystallized in hanging drops from mother liquor containing 18% w/v polyethylene glycol-monomethylether 2000, 200 mM potassium bromide and 100 mM Tris, pH 7.0, at 20 °C. Crystals grew up to 250 × 200 × 200 μm within 2 weeks. For cryoprotection crystals were briefly transferred to 8% v/v 2,3 butanediol, 18% w/v polyethylene glycol-monomethylether 2000, 500 mM potassium bromide, 100 mM Tris, pH 7.0, and flash-cooled in liquid nitrogen. Crystals displayed space group $P2_1$ (a = 85.8, b = 124.7, c = 127.4 Å, β = 95.1°), contained two molecules per asymmetric unit and diffracted to 2.4-Å resolution at European Synchrotron Radiation Facility (ESRF) beamline ID23-1. Diffraction data were processed using MOSFLM/CCP4 (24) (data statistics are presented in Table 1).

TABLE 1
Data collection and refinement statistics

Data collection	
Space group	$P2_1$
Cell dimensions	
a, *b*, *c* (Å)	85.8, 124.8, 127.4
β (°)	95.1
Resolution (Å)	33-2.4 (2.53-2.4)[a]
R_{merge} (%)	6.7 (43.5)
$I/\sigma I$	13.4 (2.4)
Completeness (%)	96.4 (98.0)
Redundancy	3.0 (2.9)
Wilson *B*-value (Å^2)	49.7
Refinement	
Resolution (Å)	33-2.4
No. reflections (F > 0σF)	95439
R_{work}/R_{free} (%)	21.3/28.1
No. atoms	
C3c	17638
Compstatin	226
Water	471
Ligand/ion	145
Average *B*-factor (Å^2)	
C3c	46.2
Compstatin	47.0
Water	39.7
Ligand/ion	57.4
r.m.s. deviations	
Bond lengths (Å)	0.011
Bond angles (°)	1.408
Ramachandran analysis (%)	
Favored regions	88.3
Additionally allowed regions	9.9
Generously allowed regions	1.8
Disallowed regions	0.8

[a] Highest resolution shell is shown in parentheses.
[b] r.m.s., root mean square.

Structure Determination—C3c-compstatin was solved by molecular replacement with Phaser (25). First C3c (Protein Data Bank code 2A74) (18) without the C345c domain was placed. Second the C345c domain of C3c was placed using Coot (26), and its position was refined by Phaser. Subsequently, all domains were refined by rigid body refinement in Phaser to account for small domain rotations and translations. Compstatin and C3c were finalized by several rounds of model building in Coot and refinement in REFMAC (24) to R and R_{free} values of 21.3% and 28.1% (Table 1). The final refined model contained 1107 residues for C3c molecule 1 (chains A, B, and C) and 1113 residues for C3c molecule 2 (chains D, E, and F). Both compstatin molecules were completely built. All molecular graphics figures were generated with PyMOL (DeLano Scientific LLC).

RESULTS

Structure of the C3c-Compstatin Complex—Here we present the structure of compstatin in complex with C3c. C3c was co-crystallized with the Ac-V4W/H9A-NH_2 analogue (Ac-ICVWQDWGAHRCT-NH_2) of compstatin (16), hereafter

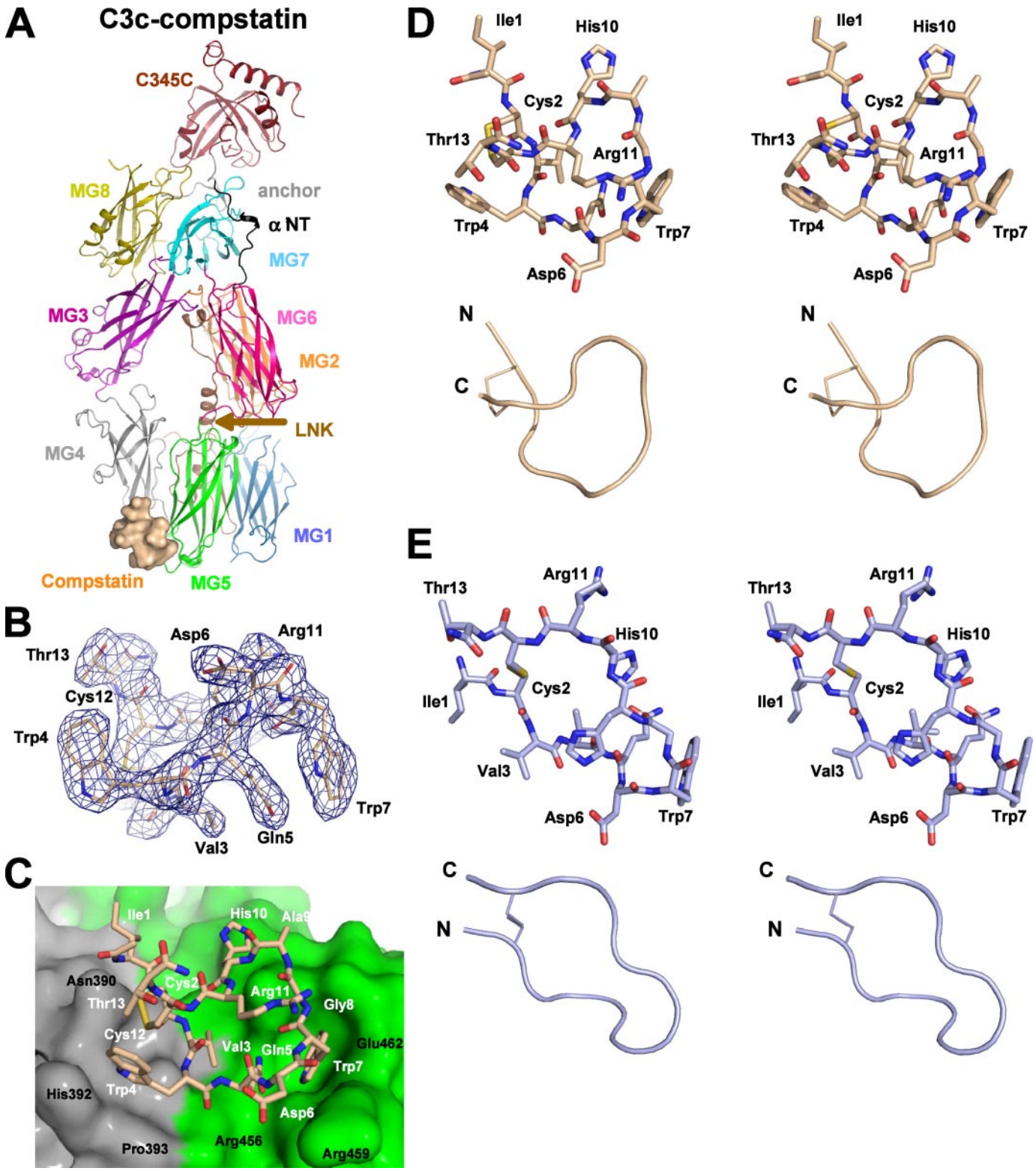

FIGURE 1. **Structure of the C3c-compstatin complex at 2.4-Å resolution.** *A*, *ribbon representation* of C3c with the bound compstatin in surface representation colored by domain and labeled accordingly. Also indicated are the anchor region (*gray*) and α′NT (*black*). *B*, electron density ($2mF_{obs} - DF_{calc}$, φ_{calc}) at 1σ of bound compstatin. *C*, compstatin-C3c interaction site with C3c in *surface representation* (*black residue numbering*) and compstatin in *stick representation* (*white residue numbering*). Colors are according to *panel A*. *D*, stereo diagram of bound compstatin in *stick representation* (*upper panel*) and in *ribbon representation* (*lower panel*) with the disulfide bond indicated. *E*, stereo diagram of free compstatin (original peptide (10)) shown in the same orientation and views as bound compstatin in *panel D*. Bound compstatin undergoes a conformational change upon binding to C3c.

referred to as compstatin. Crystals diffracted to 2.4-Å resolution and displayed space group $P2_1$. Two complexes of C3c-compstatin are present in the asymmetric unit. Complex formation agrees with the 1:1 stoichiometry determined by surface-plasmon resonance (14). The overall structures of the independent C3c-compstatin complexes are very similar. Dif-

ferences are observed in the orientation of some domains (see supplemental Table I*a*). The differences, which are the largest for C345c, MG8, MG7, and MG3 (in decreasing order), correspond with observed variations for these domains in other structures of C3 and its fragments (18, 19, 21).

The structure of the C3c-compstatin complex reveals that compstatin binds between domains MG4 and MG5 (Fig. 1). The MG4 and MG5 domains are part of the 40-kDa C-terminal fragment of the β-chain; thus, the observed binding site is in agreement with prior biochemical data (17). The β-sheets βA-βB-βE of MG4 and βA-βB-βE of MG5 form a shallow groove. Compstatin binds to the lower end of this groove. Thus, compstatin binds C3c at the bottom end of the MG-ring, far away from the α-chain.

Structure of Compstatin—Compstatin bound to C3c differs markedly in conformation from that of free compstatin (10, 16) (Fig. 1, *D* and *E*). In complex with C3c, compstatin is folded in a conformation with a β-turn formed by residues 8–11. The N and C termini point outwards and are outside of the main loop formed by residues 2–10, which is covalently closed by the disulfide bond between Cys-2 and Cys-12. Between the two complexes in the asymmetric unit, compstatin differs only in the orientation of Ile-1 and the acetylated N terminus and Arg-11 (supplemental Fig. 1). This conformation of compstatin differs from those present in the NMR ensemble of free compstatin (10, 16). Free compstatin has a β-turn at residues 5–8, whereas in bound compstatin, a β-turn at residues 8–11 is observed. The side-chain interactions between residues 3, 4, and 7 required for conformational stability of free compstatin (10, 16) are absent in bound compstatin. In contrast, residues Val-3, Trp-4, and Trp-7 are involved in hydrophobic interactions with C3c in bound compstatin. Furthermore, Trp-4 and Trp-7 in bound compstatin do not show π-π stacking interactions (16); instead, Trp-4 is involved in CH/π and sulfur-aromatic interactions with Cys-12 when bound to C3c. The root mean square (r.m.s.) deviation between free and bound compstatin after superpositioning is 3.7 Å for all 13 Cαs and 4.9 Å for all (101, non-hydrogen) atoms (27). These data show clearly that compstatin undergoes a dramatic conformational rearrangement upon binding to C3c.

Structure of C3c—The structure of C3c in complex with compstatin reveals the same overall domain arrangement of 10 domains as observed for free C3c (18). For most domains, we observe small variations in domain orientation among the two structures of C3c-compstatin and the two structures of free C3c in the asymmetric unit (see supplemental Table I*b*). Large differences are observed for C345c (up to 15.4° rotation) and MG8 (up to 8.3° rotation). These differences reflect the flexibility of the C3c molecule. Differences in domain orientation of MG4 and MG5 within C3c range from 2.4 to 3.6° and 1.4 to 1.9°, respectively. The relative orientations between MG4 and MG5 differ by only 4.2° among these structures of C3c. These data indicate that compstatin does not affect the overall domain arrangement of C3c.

Compstatin-C3c Interactions—Compstatin interacts extensively with C3c. One side of the compstatin-loop structure faces C3c, and one side faces the solvent with residues 2–9 alternating inside and outside. Residues 11–13 extend outward away

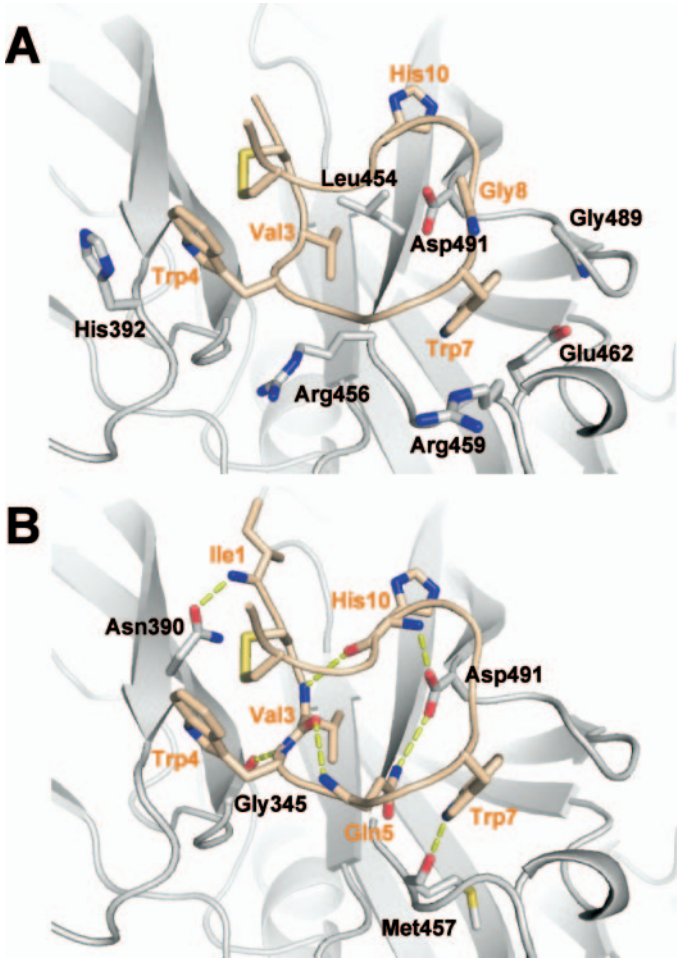

FIGURE 2. **Interactions between C3c and compstatin.** C3c is colored *gray*, and compstatin is colored as in Fig. 1*A*. *A*, residues involved in van der Waals contact, observed in both complexes within the asymmetric unit of the crystal, are shown in *stick representation*. *B*, hydrogen bonds between C3c and compstatin and within compstatin itself, observed in both complexes within the asymmetric unit, are shown by *yellow dotted lines*. See supplemental Table II for all observed contacts between C3c and compstatin.

from C3c. In total, 40% of the molecular surface of compstatin is buried in the complex, resulting in 1120 Å^2 buried surface area of the complex. The interface of compstatin with C3c is characterized by both hydrophobic and hydrophilic interactions (see supplemental Table II). Notably, Val-3 and the Trp-7 of compstatin are buried in hydrophobic pockets formed by C3c residues Met-346, Pro-347, Leu-454, Arg-456 and Leu-455, Arg-456, Arg-459, and Glu-462, respectively (Figs. 1*C* and 2*A*). A hydrogen-bonding network between both backbone and side-chain atoms of C3c and compstatin further stabilize the interaction (supplemental Table IIa and Fig. 2*B*). A small difference in bound waters is observed in the interface of compstatin with C3c between the two complexes in the asymmetric unit. In one complex (chains A, B, and C for C3c and chain G for compstatin in the deposited Protein Data Bank file), we observe no bound water molecule, whereas in the other complex (chains D, E, and F and chain H, respectively), we observe two water molecules mediating hydrogen bonding between compstatin and C3c. The water molecules mediate interactions between compstatin Gln-5 and C3c Asp-491 and the backbone carbonyl oxygens of

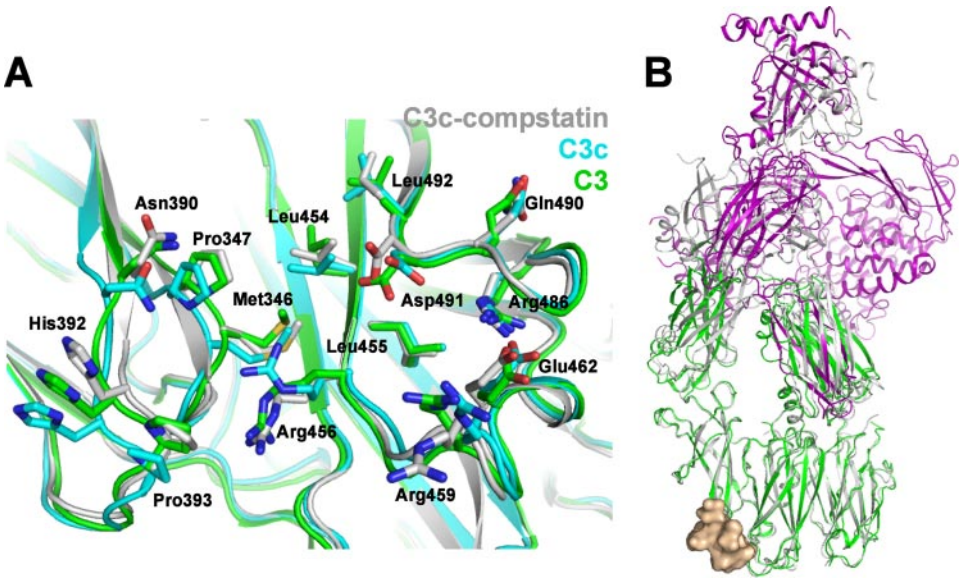

FIGURE 3. **Comparison of C3c-compstatin, C3c and C3.** *A*, ribbon representation of the compstatin-binding site with C3c-compstatin (*gray*), C3c (*cyan*) (18), and C3 (*green*) (18) superposed using domain MG4 and MG5 (24). Compstatin is omitted for clarity. Residues involved in compstatin binding are shown in *stick representation* and are *numbered*. In the compstatin-binding site, free C3 resembles the C3c-compstatin complex more than free C3c. *B*, C3c-compstatin superposed onto C3 on the basis of MG1, MG2, and MG4-MG6 of the MG-ring (24). C3c (*gray*) and C3 (β-chain, *green*, and α-chain, *purple*) are shown in *ribbon representation*, and compstatin (*wheat*) is shown in *surface representation*. The MG4-MG5 domain orientation is conserved between C3c-compstatin and C3; therefore, compstatin binds C3 without affecting large structural changes.

compstatin Cys-2 and C3c Thr-391. This small difference in bound waters possibly reflects flexibility and small differences in crystal packing in the vicinity of the compstatin-binding site. Alternatively, we possibly have not observed all bound water molecules due to the limited resolution of 2.4 Å. For both complexes, we observe a bromide ion bound in the interface. This ion forms hydrogen bonds with the backbone nitrogen of compstatin Asp-6 and backbone nitrogen of C3c Arg-459. The crystallization solution contained 200 mM KBr, whereas the cryo-protectant contained 500 mM KBr. Possibly, the stabilizing role of bromide is replaced by a water molecule in conditions without bromide present.

Comparison of C3c-Compstatin with C3—Several structures of C3 and its fragments C3b and C3c are now available (18, 19, 21). Comparison of the medium with high resolution structures of C3, C3c, C3c-CRIg, and C3c-compstatin shows that the MG4-MG5 domain orientation is conserved (Fig. 3). Difference in orientations of other domains, notably C345c, MG8, MG7, and MG3, can be attributed to inherent flexibility of the molecule. However, we observe significant differences in the compstatin-binding site. The loop βE-βF of MG4 and positions of amino acid side chains differ up to 4.6 Å between C3c-compstatin and free C3c (Fig. 3*A*). Surprisingly, the positions of the side chains in the C3c-compstatin complex resemble more free C3 than free C3c; see, for example, the positions of Asn-390, His-392, and Pro-393 of loop βE-βF and Pro-347 and Arg-456 in Fig. 3*A* (see r.m.s. deviation values in supplemental Table I*c*). These differences between C3, C3c-compstatin, and C3c may explain the higher affinity of compstatin for C3 (K_d of 0.14 μM) than for C3c (K_d of 0.39 μM)[4] (14, 15). Overall, we may conclude that compstatin binding does not induce large rearrangements in C3c, but minor, local induced effects are present in the vicinity of the compstatin-binding site.

DISCUSSION

Compstatin Binding to C3—The crystal structure of the C3c-compstatin complex reveals that compstatin binds C3c between domains MG4 and MG5 of the β-chain. Compstatin undergoes a large conformational change upon binding to C3c. In contrast, C3c does not undergo large changes upon complex formation. The conformation of the compstatin-binding site in C3c is structurally very similar to that observed in the structure of uncomplexed C3.

The observed compstatin-binding site is supported by biochemical data. Recently, the compstatin-binding site was found to reside on the 40-kDa C-terminal region of the β-chain of C3 (17). Both domains MG4 and MG5 are part of this region. Compstatin displays species specificity; it binds only to primate C3 and not to C3 from lower mammalian species (28). Residues Gly-345, His-392, Pro-393, Leu-454, and Arg-459 are all extensively involved in interactions with compstatin, as determined by the crystal structure. These residues are conserved in primate C3, whereas they all differ in other mammals (see supplemental Fig. 2). These different amino acid residues would yield steric hindrance or lead to loss of specific interactions, and, thus explain the species specificity observed for compstatin.

The structure of compstatin in the C3c-compstatin complex differs markedly from the structure of compstatin in solution. Previous activity data from mutational studies, however, are in agreement with the observed C3c-compstatin complex. These studies indicated that the disulfide bridge, residues in the β-turn (residues 5–8), and some residues in the hydrophobic cluster at the linked termini (residues 1–4 and 12–13) were essential for binding to C3 (10, 13, 14). Both main-chain and side-chain atoms were proposed to be directly involved in binding to C3 (11, 14, 28). More specifically, hydrophobic residues Val-3 and Trp-7 were shown to be essential for activity. The indole amide of Trp-7 was proposed to be involved in hydrogen bonding with C3 (10, 11, 29); in contrast, the indole amide of Trp-4 was not (29). In our crystal structure, both main-chain and side-chain atoms contribute to the compstatin-C3c interactions, residues 2 and 3 of the hydrophobic cluster are involved in hydrophobic interaction with C3c, Val-3 and Trp-7 have extensive hydrophobic interactions with C3c, and the amide indole of Trp-7 forms a hydrogen bond with the main-chain oxygen of Met-457 (see also supplemental Table II), whereas the amide indole of Trp-4 does not form a hydrogen bond with

[4] M. Katragadda and J. D. Lambris, unpublished results.

C3c. Thus, many of the previously proposed interactions are in agreement with the structure of the C3c-compstatin complex.

Isothermal titration calorimetry experiments indicated that the C3-compstatin binding is an enthalpy-driven process (15). It was proposed that the unfavorable entropy could arise from binding water molecules at the interface or could be due to conformational changes in C3 and/or compstatin (15). We observe large structural differences between free and bound compstatin. In contrast, only small structural differences are observed in the compstatin-binding site region between structures of C3, C3c (18), and C3c-compstatin (Fig. 3). We observe very few water molecules mediating the interactions between compstatin and C3c; this fits with the tight packing and the amount of hydrophobic interactions observed in the complex. Therefore, we conclude that the observed unfavorable entropy of complex formation arises mostly from the conformational change that compstatin undergoes upon binding to C3.

Compstatin's Mode of Action—Two possible mechanisms for complement inhibition by compstatin have been proposed; compstatin either (i) sterically hinders binding of C3 to the convertase or (ii) induces conformational changes in C3, preventing binding of C3 to the convertase. Our data clearly show that the binding site of compstatin lies far away from any other known binding site on C3 or its proteolytic fragments (30) and that compstatin binds C3 without effecting large structural changes. These data are consistent with the observation that compstatin does not interfere with the formation of the C3 convertase or with the function of any of the complement regulatory proteins (6). In addition, binding of compstatin to C3 does not increase protease sensitivity (6), in contrast to bacterial protein extracellular fibrinogen-binding protein (Efb-C), which affects protease sensitivity by changing the conformation of C3 (31). The effect observed by surface plasmon resonance and isothermal titration calorimetry suggested that conformational changes play an important role in compstatin-C3 binding (14, 15). We argue that the marked conformational change of compstatin suffices to explain the surface plasmon resonance and isothermal titration calorimetry results. We therefore conclude that compstatin does not act by changing the conformation of C3 but likely acts through sterically hindering the binding of C3 to the convertase.

How does compstatin sterically hinder C3 binding to the convertases? Most binding sites for interacting proteins have been mapped to the α-chain of C3 (30). The exception is the recently identified complement receptor CRIg, which also inhibits convertase activity (21). Crystal structures revealed that CRIg binds C3b and C3c predominantly at domains MG3 and MG6 of the β-chain (21). Compstatin binds C3 between domains MG4 and MG5. These two binding sites of CRIg and compstatin are >20 Å apart but lie on the same face of the MG-ring of the β-chain. Interestingly, in the crystal of C3b, we observe a C3b-C3b crystallographic symmetry-related contact site formed by the same face of the MG-ring (Fig. 4*A*) (19). We hypothesize that this MG-ring interaction face may indicate a major exosite in substrate binding forming the C3-C3bBb substrate-enzyme complex. Both CRIg and compstatin would sterically hinder the formation of this interface of the substrate-enzyme complex, and thus, explain the inhibitory activity of

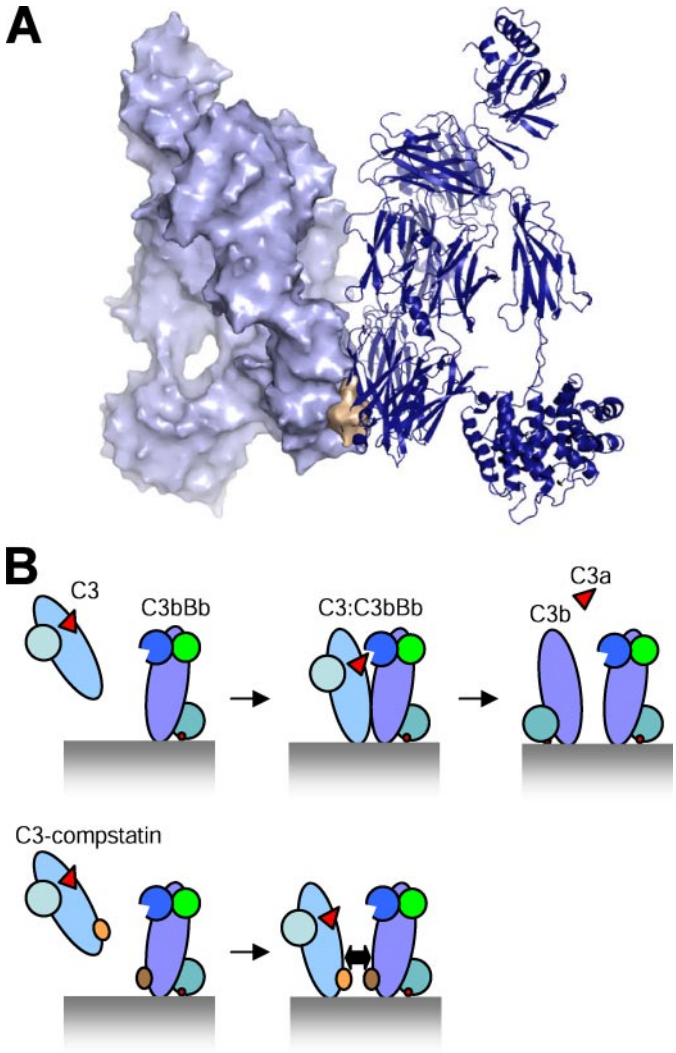

FIGURE 4. **Model for inhibition by compstatin.** *A*, two symmetry-related molecules of C3b contact each other at the compstatin-binding site in the crystal of C3b (19). Compstatin (*wheat*) is superposed onto a C3b molecule (*surface representation*) on the basis of the C3c-compstatin structure. The symmetry related C3b molecule (*ribbon representation*) clashes severely with compstatin. *B*, *top diagram*, schematic representation of the back-to-back binding of C3 to the convertase (based on crystal structures of C3 (18), C3b (19, 21), and factor Bb (33)). *Bottom diagram*, schematic representation of steric hindrance of C3 binding to the convertase induced by compstatin.

both molecules (Fig. 4*B*). Compstatin may also bind the enzyme complex, C3bBb (6). In our back-to-back model of the MG-ring interaction in C3-C3bBb substrate-enzyme complex, compstatin might inhibit the interaction both ways, either through binding the substrate or through binding the enzyme complex. This additional mechanism may explain the higher inhibitory activity of compstatin in the alternative pathway when compared with the classical pathway (6, 12). In the classical pathway, compstatin can only bind to C3 and not to the convertase C4bC2a (28), whereas in the alternative pathway, compstatin can bind both the substrate C3 and the convertase C3bBb, thus possibly acting in a dual way. Thus, based on an interaction surface observed in C3b crystals and the interaction sites of compstatin and CRIg, we propose a model for C3 binding to the convertase. This model explains how a small peptide inhibitor, compstatin, has the same inhibitory effect as the large protein receptor CRIg.

We have identified that the potential therapeutic compstatin binds C3 on a shallow groove between two domains of the β-chain. Most drug design projects target well defined pockets in proteins for binding low molecular weight inhibitors to achieve high binding affinity and specificity. Remarkably, compstatin binds on a rather flat surface of the C3c molecule. Nevertheless, it has been possible to improve the specific activity by structure-activity studies and experimental and theoretical combinatorial approaches (reviewed in Ref. 32). The structure of the complex between C3c and compstatin provides crucial information on the bound conformation of compstatin and the binding site on C3. These data provide new impetus to develop improved and less costly non-peptide inhibitors, for example, by developing molecules that structurally mimic the bound form of compstatin. The detailed knowledge of the binding site provides the possibility to develop a mouse model by conservatively "humanizing" mouse C3 to enable *in vivo* testing of complement inhibition of compstatin and derivatives in various complement disease models. Finally, the current data indicate a potential role for the large MG-ring of the β-chain in substrate binding to the convertase.

Acknowledgments—We acknowledge the European Synchrotron Radiation Facility for provision of synchrotron radiation facilities and we would like to thank Xavier Thibault for assistance in using beamline ID23-1. We thank Daniel Ricklin and Serapion Pyrpassopoulos for comments.

REFERENCES

1. Walport, M. J. (2001) *N. Engl. J. Med.* **344,** 1058–1066
2. Carroll, M. C. (2004) *Nat. Immunol.* **5,** 981–986
3. Sahu, A., and Lambris, J. D. (2000) *Immunopharmacology* **49,** 133–148
4. Bureeva, S., Andia-Pravdivy, J., and Kaplun, A. (2005) *Drug Discov. Today* **10,** 1535–1542
5. Holland, M. C., Morikis, D., and Lambris, J. D. (2004) *Curr. Opin. Investig. Drugs* **5,** 1164–1173
6. Sahu, A., Kay, B. K., and Lambris, J. D. (1996) *J. Immunol.* **157,** 884–891
7. Fiane, A. E., Mollnes, T. E., Videm, V., Hovig, T., Hogasen, K., Mellbye, O. J., Spruce, L., Moore, W. T., Sahu, A., and Lambris, J. D. (1999) *Xenotransplantation* **6,** 52–65
8. Nilsson, B., Larsson, R., Hong, J., Elgue, G., Ekdahl, K. N., Sahu, A., and Lambris, J. D. (1998) *Blood* **92,** 1661–1667
9. Soulika, A. M., Khan, M. M., Hattori, T., Bowen, F. W., Richardson, B. A., Hack, C. E., Sahu, A., Edmunds, L. H., Jr., and Lambris, J. D. (2000) *Clin. Immunol.* **96,** 212–221
10. Morikis, D., Assa-Munt, N., Sahu, A., and Lambris, J. D. (1998) *Protein Sci.* **7,** 619–627
11. Morikis, D., Roy, M., Sahu, A., Troganis, A., Jennings, P. A., Tsokos, G. C., and Lambris, J. D. (2002) *J. Biol. Chem.* **277,** 14942–14953
12. Furlong, S. T., Dutta, A. S., Coath, M. M., Gormley, J. J., Hubbs, S. J., Lloyd, D., Mauger, R. C., Strimpler, A. M., Sylvester, M. A., Scott, C. W., and Edwards, P. D. (2000) *Immunopharmacology* **48,** 199–212
13. Soulika, A. M., Morikis, D., Sarrias, M. R., Roy, M., Spruce, L. A., Sahu, A., and Lambris, J. D. (2003) *J. Immunol.* **171,** 1881–1890
14. Sahu, A., Soulika, A. M., Morikis, D., Spruce, L., Moore, W. T., and Lambris, J. D. (2000) *J. Immunol.* **165,** 2491–2499
15. Katragadda, M., Morikis, D., and Lambris, J. D. (2004) *J. Biol. Chem.* **279,** 54987–54995
16. Mallik, B., Katragadda, M., Spruce, L. A., Carafides, C., Tsokos, C. G., Morikis, D., and Lambris, J. D. (2005) *J. Med. Chem.* **48,** 274–286
17. Soulika, A. M., Holland, M. C., Sfyroera, G., Sahu, A., and Lambris, J. D. (2006) *Mol. Immunol.* **43,** 2023–2029
18. Janssen, B. J., Huizinga, E. G., Raaijmakers, H. C., Roos, A., Daha, M. R., Nilsson-Ekdahl, K., Nilsson, B., and Gros, P. (2005) *Nature* **437,** 505–511
19. Janssen, B. J., Christodoulidou, A., McCarthy, A., Lambris, J. D., and Gros, P. (2006) *Nature* **444,** 213–216
20. Fredslund, F., Jenner, L., Husted, L. B., Nyborg, J., Andersen, G. R., and Sottrup-Jensen, L. (2006) *J. Mol. Biol.* **361,** 115–127
21. Wiesmann, C., Katschke, K. J., Yin, J., Helmy, K. Y., Steffek, M., Fairbrother, W. J., McCallum, S. A., Embuscado, L., DeForge, L., Hass, P. E., and van Lookeren Campagne, M. (2006) *Nature* **444,** 217–220
22. Nishida, N., Walz, T., and Springer, T. A. (2006) *Proc. Natl. Acad. Sci. U. S. A.* **103,** 19737–19742
23. Bokisch, V. A., Muller-Eberhard, H. J., and Cochrane, C. G. (1969) *J. Exp. Med.* **129,** 1109–1130
24. Collaborative Computational Project Number 4 (1994) *Acta Crystallogr. Sect. D Biol. Crystallogr.* **50,** 760–763
25. McCoy, A. J., Grosse-Kunstleve, R. W., Storoni, L. C., and Read, R. J. (2005) *Acta Crystallogr. Sect. D Biol. Crystallogr.* **61,** 458–464
26. Emsley, P., and Cowtan, K. (2004) *Acta Crystallogr. Sect. D Biol. Crystallogr.* **60,** 2126–2132
27. Kleywegt, G. J. (1996) *Acta Crystallogr. Sect. D Biol. Crystallogr.* **52,** 842–857
28. Sahu, A., Morikis, D., and Lambris, J. D. (2003) *Mol. Immunol.* **39,** 557–566
29. Katragadda, M., Magotti, P., Sfyroera, G., and Lambris, J. D. (2006) *J. Med. Chem.* **49,** 4616–4622
30. Janssen, B. J., and Gros, P. (2007) *Mol. Immunol.* **44,** 3–10
31. Hammel, M., Sfyroera, G., Ricklin, D., Magotti, P., Lambris, J. D., and Geisbrecht, B. V. (2007) *Nat. Immunol.* **8,** 430–437
32. Morikis, D., Soulika, A. M., Mallik, B., Klepeis, J. L., Floudas, C. A., and Lambris, J. D. (2004) *Biochem. Soc. Trans.* **32,** 28–32
33. Ponnuraj, K., Xu, Y., Macon, K., Moore, D., Volanakis, J. E., and Narayana, S. V. (2004) *Mol. Cell* **14,** 17–28